vious work.[6,11] In the molecular model, L is a two electron donor, *i.e.*, CO or H^-. All Tl-Tl, Tl-Fe, Fe-C, Fe-H, and C-O distances were fixed at 3.75, 2.67, 1.78, 1.60, and 1.14 Å, respectively. The L-Fe-L angles were fixed at 90.0°.

References

1. (a) B. F. G. Johnson, "Transition Metal Clusters", Wiley, Chichester, 1980; (b) Ch. Elschenbroich and A. Salzer, "Organometallics", VCH, Weinheim, 1992.
2. T. A. Albright, J. K. Burdett, and M.-H. Whangbo, "Orbital Interactions in Chemistry", Wiley, New York, 1985.
3. (a) J. K. Burdett, "Molecular shapes", Wiley, New York 1980; (b) K. Wade, *Adv. Inorg. Chem. Radiochem.,* **18**, 1 (1976); (c) D. M. P. Mingos, *Inorg. Chem.,* **24**, 114 (1985); (d) B. K. Teo, *Inorg. Chem.,* **24**, 1627 (1985); (e) W. N. Lipscomb, "In Born Hydride Chemistry", E. L. Muetterties, Ed., Academic Press, New York, pp. 39, 1975.
4. K. H. Whitmire, R. R. Ryan, H. J. Wasserman, T. A. Albright, and S. K. Kang, *J. Am. Chem. Soc.,* **108**, 6831 (1986).
5. (a) J. Beck and J. Strähle, *Z. Naturforsch,* **41b**, 1381 (1986); (b) S. Harvey, M. F. Lappert, C. L. Raston, B. W. Skelton, G. Strivastava, and A. H. White, *J. Chem.*

Soc., Chem. Commun., 1216 (1988); (c) K. H. Whitmire, J. M. Cassidy, A. L. Rheingold, and R. R. Ryan, *Inorg. Chem.,* **27**, 1347 (1988); (d) J. M. Cassidy and K. H. Whitmire, *Inorg. Chem.,* **28**, 1432 (1989).
6. C. Janiak and R. Hoffmann, *J. Am. Chem. Soc.,* **112**, 5924 (1990).
7. (a) T. A. Albright, *Tetrahedron,* **38**, 1339 (1982); (b) K. H. Whitmire, T. A. Albright, S. K. Kang, M. R. Churchill, and J. C. Fettinger, *Inorg. Chem.,* **25**, 2799 (1986); (c) J. A. S. Howell, N. F. Ashford, D. T. Dixon, J. C. Kola, T. A. Albright, and S. K. Kang, *Organometallics,* **10**, 1852 (1991).
8. (a) M. R. Churchill, F. J. Hollander, and J. P. Hutchinson, *Inorg. Chem.,* **16**, 2655 (1977); (b) M. R. Churchill and B. G. DeBoer, *Inorg. Chem.,* **16**, 878 (1977); (c) L. F. Dahl and J. F. Blount, *Inorg. Chem.,* **4**, 1965 (1965).
9. R. Hoffmann, *J. Chem. Phys.,* **39**, 1397 (1963); R. Hoffmann and W. N. Lipscomb, *J. Chem. Phys.,* **36**, 2179 (1962); **37**, 2872 (1962).
10. J. H. Ammeter, H.-B. Bürgi, J. C. Thibeault, and R. Hoffmann, *J. Am. Chem. Soc.,* **100**, 3686 (1978).
11. T. A. Albright, P. Hofmann, and R. Hoffmann, *J. Am. Chem. Soc.,* **99**, 7546 (1977).

Dioxygen Binding to Dirhodium(II, II), (II, III), and (III, III) Complexes. Spectroscopic Characterization of $[Rh_2(ap)_4(O_2)]^+$, $Rh_2(ap)_4(O_2)$, and $[Rh_2(ap)_4(O_2)]^-$, where ap=2-anilinopyridinate Ion

Jae-Duck Lee*, Chao-Liang Yao, Francoise J. Capdevielle, Baocheng Han, John L. Bear†, and Karl M. Kadish†

Department of Chemistry, University of Houston, Houston, Texas 77204-5641, U.S.A.
Received September 9, 1992

The neutral, reduced, and oxidized 2,2-trans isomers of $Rh_2(ap)_4$ (ap=2-anilinopyridinate) were investigated with respect to dioxygen binding in CH_2Cl_2 containing 0.1 M tetrabutyl-ammonium perchlorate. $Rh_2(ap)_4$ binds dioxygen in nonaqueous media and forms a $Rh^{II}Rh^{III}$ superoxide complex, $Rh_2(ap)_4(O_2)$. This neutral species was isolated and is characterized by UV-visible and IR spectroscopy, mass spectrometry and cyclic voltammetry. It can be reduced by one electron at $E_{1/2}=-0.45$ V vs. SCE in CH_2Cl_2 and gives $[Rh_2(ap)_4(O_2)]^-$ as demonstrated by the ESR spectrum of a frozen solution taken after controlled potential reduction. The superoxide ion in $[Rh_2(ap)_4(O_2)]^-$ is axially bound to one of the two rhodium ions, both of which are in a +2 oxidation state. $Rh_2(ap)_4(O_2)$ can also be stepwise oxidized in two one-electron transfer steps at $E_{1/2}=0.21$ V and 0.85 V vs. SCE in CH_2Cl_2 and gives $[Rh_2(ap)_4(O_2)]^+$ followed by $[Rh_2(ap)_4(O_2)]^{2+}$. ESR spectra demonstrate that the singly oxidized complex is best described as $[Rh^{II}Rh^{III}(ap)_4(O_2)]^+$ where the odd electron is delocalized on both of the two rhodium ions and the axial ligand is molecular oxygen.

Introduction

$Rh_2(ap)_4$ (where ap=2-anilinopyridiate) can exist in four different isomeric forms, two of which have been isolated and structurally characterized.[1,2] The 4.0 isomer has one rhodium ion bound by four anilino nitrogens and the other by four pyridyl nitrogens. In contrast, each rhodium atom of the $Rh_2(ap)_4$ 2,2-trans isomer is bound in a *trans* fashion

by two pyridyl nitrogens and two anilino nitrogens of the bridging ligands.

Our laboratory recently reported electrochemical properties of the 4,0 isomer in the presence of O_2 and demonstrated the formation of $Rh^{II}Rh^{III}(ap)_4(O_2)$, where the dioxygen ligand was bound to the rhodium ion which was complexed by the four pyridyl nitrogens.[3] The 2,2-*trans* isomer of Rh_2, whose structure is shown in Fiugre 1, will also irreversibly bind dioxygen and gives a stable $Rh_2(ap)_4(O_2)$ complex in CH_2Cl_2 or THF solutions under O_2. This complex was isola-
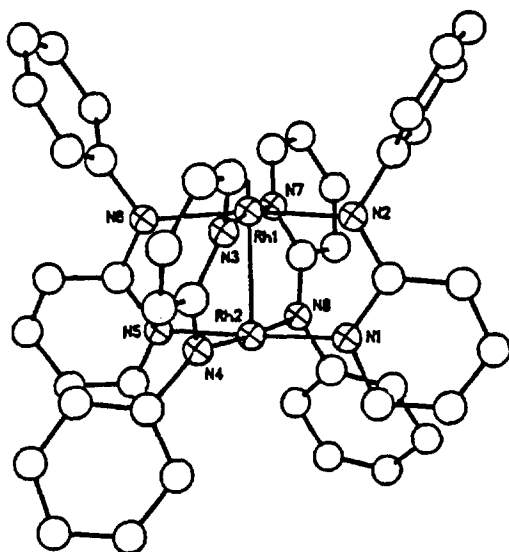
Figure 1. Structural view of the $Rh_2(ap)_4$ 2,2-*trans* isomer.

Figure 2. (a) UV-visible spectral changes and (b) analysis of the data for the binding of O_2 by 4.2×10^{-4} M $Rh_2(ap)_4$ in CH_2Cl_2 under 1 atm O_2.

ted and is characterized by UV-visible and IR spectroscopy, mass spectrometry and cyclic voltammetry. Stable $[Rh_2(ap)_4 (O_2)]^-$ or $[Rh_2(ap)_4(O_2)]^+$ species may also be generated by electrochemical reduction or oxidation of $Rh_2(ap)_4(O_2)$. This is demonstrated in the present paper, where the dioxygen complexes of Rh^{II}_2, $Rh^{II}Rh^{III}$, and Rh^{III}_2 are characterized by UV-visible, IR or ESR spectroscopy and their properties discussed with respect to both the metal oxidation state and the nature of the bound O_2 or O_2^- ligand.

Experimental Section

Solvents and Reagents. Synthesis and purification of the $Rh_2(ap)_4$ 2,2-*trans* isomer was carried out as reported in the literature.[12] $Rh_2(ap)_4(O_2)$ was synthesized by bubbling O_2 into a solution of $Rh_2(ap)_4$ in CH_2Cl_2 overnight and then purified on a silica gel column using a 1 : 10 ether/CH_2Cl_2 mixture. The first eluted species was yellow green and was collected for further analysis. Spectroscopic grade CH_2Cl_2 was purified by distillation over CaH_2. Tetrahydrofuran (THF) was distilled from CaH_2 followed by distillation over Na/ben-zophenone under N_2. The supporting electrolyte, tetra-*n*-butyl-ammonium perchlorate (TBAP), was twice recrystallized from absolute ethanol. Ultrahigh purity grade O_2 was purchased from Big Three, Inc. and contained a maximum of 3 ppm H_2O.

Instrumentation. A three-electrode system was used for cyclic voltammetric exeriments and consisted of a Pt-button working electrode, a Pt-wire auxiliary electrode and a saturated calomel reference electrode (SCE). All potentials are reported *vs.* the SCE.

An IBM Model 225 voltammetric analyzer was used to record the cyclic voltammograms and a BAS SP-2 potentio-stat was used to perform controlled-potential electrolysis. ESR spectra were recorded on an IBM Model 100D ESR spectrometer. IR spectra of the neutral complexes were measured on an IBM Model IR/32 FTIR spectrometer and had a ± 2 cm^{-1} resolution. Mass spectra were obtained from a high-resolution hybrid tandem VG Analytical Model 70-SEQ
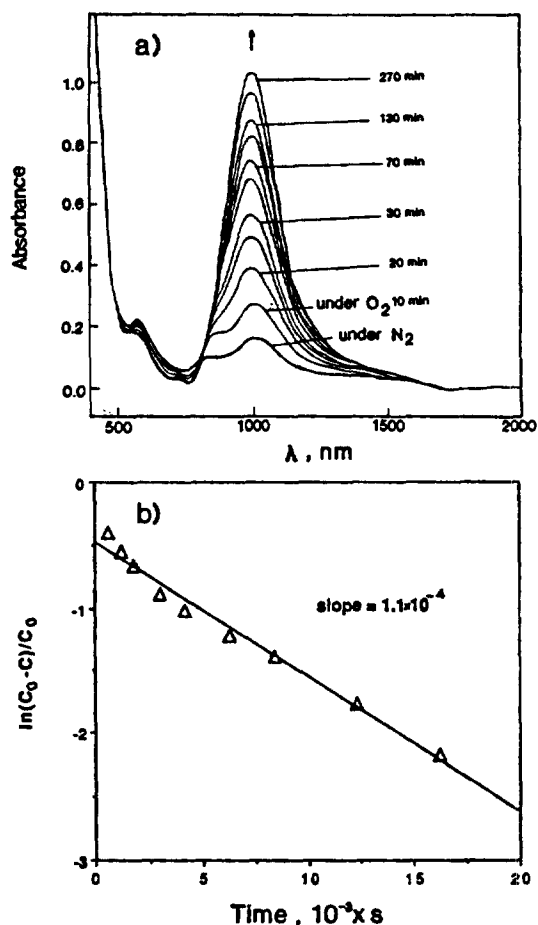
spectrometer (EEQQ geometry). A standard fast atom bombardment (FAB) source was utilized and *m*-nitrobenzyl alcohol (NBA) was used as the liquid matrix. UV-visible spectra were recorded on a Perkin-Elmer 330 spectrophotometer with a 1.0 cm path length cell.

Results and Disussion

Spectroscopic Characterization of $Rh_2(ap)_4(O_2)$.
The color of $Rh_2(ap)_4$ in CH_2Cl_2 changes slowly from green to brown when the N_2 gas over the solution is replaced by O_2. Similar color changes are observed in THF but not in CH_3CN which strongly coordinates to the dirhodium center.[13] This color change is consistent with the formation of a Rh^{II}-Rh^{III} complex[3] and/or coordination of O_2 by $Rh_2(ap)_4$ in non-bonding media as shown in reaction 1.

$$Rh_2(ap)_4 + O_2 \rightarrow Rh_2(ap)_4(O_2) \qquad (1)$$
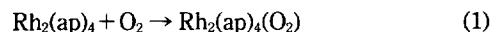
The above reaction is irreversible and the $Rh_2(ap)_4(O_2)$ spectrum remains unchanged when the O_2 atmosphere is replaced by N_2 above the solution.

The conversion of $Rh_2(ap)_4$ to $Rlh_2(ap)_4(O_2)$ was monitored by UV-visible spectroscopy and gives the time resolved UV-visible data shown in Figure 2a. This experiment was carried out under 1 atm O_2 in order to ensure as constant concentra-
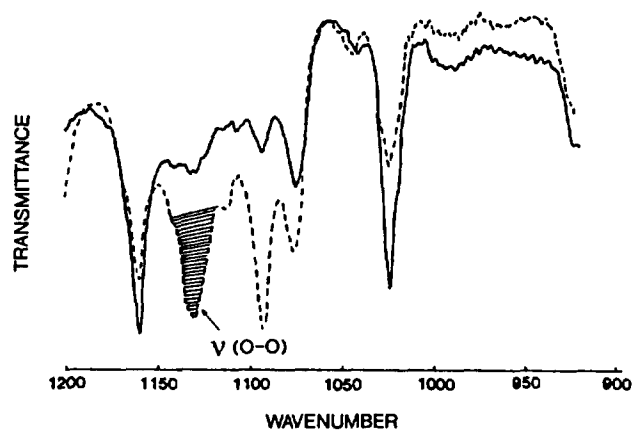
Figure 3. IR spectra of Rh₂(ap)₄ under N₂ (—) and under O₂ (%) in CH₂Cl₂.

Figure 4. Cyclic voltammograms of (a) Rh₂(ap)₄ under Ar, (b) Rh₂(ap)₄ under O₂ and (c) Rh₂(ap)₄(O₂) under Ar in CH₂Cl₂ containing 0.1 M TBAP. Scan rate=0.1 V/s.

tion of dissolved O₂ in solution. Under these experimental conditions the reaction rate is pseudo-first order with respect to the dirhodium complex (see Figure 2b). The rate constant for the reaction between Rh₂(ap)₄ and O₂ can be obtained from the slope of the line in Figure 2b and gives a value of 1.1×10^{-4} sec^{-1}P$_{O_2}^{-1}$, which is about 3 orders of magnitude slower than for reaction of the 4,0 isomer with O₂ in CH₂Cl₂.[3]

The four bridging 2-anilinopyridine ligands in the 2,2-*trans* isomer create an identical axial and equatorial environment around both rhodium ions in Rh₂(ap)₄. The complex is not polarized and has been unambiguously assigned as containing a Rh$^{II}_2$ nucleus.[1,2] Howerver, the metal oxidation state assignment in Rh₂(ap)₄(O₂) will depend upon whether bound dioxygen is in the form of neutral O₂ or in the form of negatively charged O₂$^-$. The O₂ adduct should contain Rh$^{II}_2$, while the O₂$^-$ adduct should contain Rh^{II}Rh^{III}.

The formation of a superoxide complex in Rh₂(ap)₄(O₂) and a definitive assignment of the rhodium ion oxidation state in this complex is given by the UV-visible and IR spectra. The UV-visible spectrum of Rh$^{II}_2$(ap)₄ in CH₂Cl₂ under N₂ does not display any strong absorption above 600 nm and can be contrasted with the spectrum of [Rh^{II}Rh^{III}(ap)₄]$^-$ which has a broad near-IR absorption at 1045 nm (ε=6.1× 10³) and a shoulder at 1470 nm under the same solution conditions.[1] The spectrum of Rh₂(ap)₄ in CH₂Cl₂ under O₂ has a strong absorption at 1004 nm (ε=3.9×10³) and a shoulder at 1440 nm. The overall shape of this spectrum is similar[1] to that of [Rh^{II}Rh^{III}(ap)₄]$^+$.

The IR spectra of Rh₂(ap)₄ and Rh₂(ap)₄(O₂) in CH₂Cl₂ are shown in Figure 3. Rh₂(ap)₄ under N₂ (solid line, Figure 3) has peaks at 1160, 1074, and 1023 cm^{-1} but new IR bands are observed at 1131 and 1093 cm^{-1} when the same solutions is saturated with pure oxygen (dashed line, Figure 3). Similar spectral changes are also found for Rh₂(ap)₄ and Rh₂(ap)₄(O₂) in the solid state. The solid IR spectrum of the isolated product shows two new peaks at 1093 and 1116 cm^{-1} and these suggest the formation of a metal-superoxide complex.[4] The UV-visible spectrum of the isolated product in CH₂Cl₂ is also identical to the spectrum in Figure 2. Thus, the combined UV-visible and IR data for this species indicate that the two rhodium ions of Rh₂(ap)₄(O₂) have a formal Rh^{II}Rh^{III} oxidation state and the O₂ is present as an axially-coordinated superoxide ion. Furthermore, the mass spectral data clearly indi-
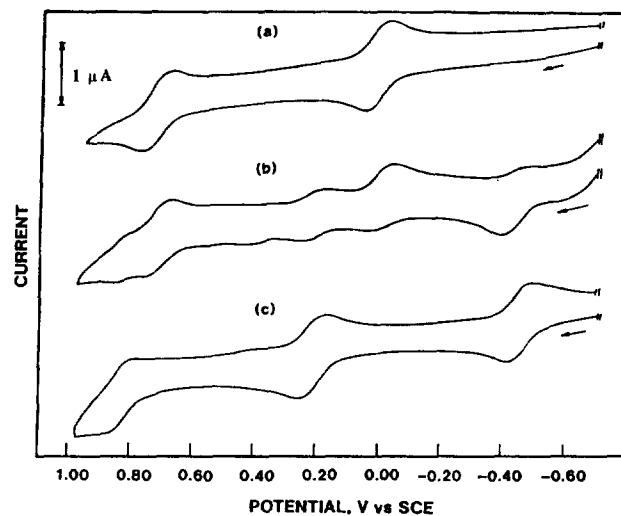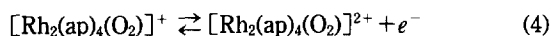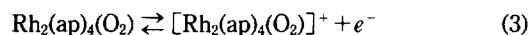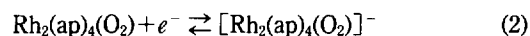
cates the formation of Rh₂(ap)₄(O₂). Both the parent peak of Rh₂(ap)₄(O₂) (at m/e=914) and the fragment of Rh₂(ap)₄(O) (m/e=898) are observed.

Electrochemical Generation of [Rh₂(ap)₄(O₂)]$^-$ and [Rh₂(ap)₄(O₂)]$^+$ in CH₂Cl₂. Cyclic voltammograms of Rh₂ (ap)₄ in CH₂Cl₂, 0.1 M TBAP under Ar show oxidations at $E_{1/2}$=0.05 and 0.83 V and these reactions correspond[1] to the successive formation of [Rh^{II}Rh^{III}(ap)₄]$^+$ and [Rh$^{III}_2$(ap)₄]$^{2+}$.

The bubbling of oxygen through solutions of Rh₂(ap)₄ in CH₂Cl₂ results in a new reduction at $E_{1/2}$= −0.45 V as well as two new oxidations at $E_{1/2}$=0.21 V and 0.85 V. The 4, 0 isomer of Rh₂(ap)₄ in CH₂Cl₂ under O₂ undergoes a similar reduction at E$_{1/2}$= −0.48 V and this process was assigned[3] as leading to the formation of [Rh₂(ap)₄(O₂)]$^-$. Thus, the fact that the two isomers of Rh₂(ap)₄ have similar voltammograms further confirms the formation of an O₂ adduct for the 2,2-*trans* isomer in CH₂Cl₂.

The electrochemical data suggests that two oxidations of Rh₂(ap)₄(O₂) generate first [Rh₂(ap)₄(O₂)]$^+$ and the [Rh₂(ap)₄ (O₂)]$^{2+}$ and the cyclic voltammogram of isolated Rh₂(ap)₄(O₂) in CH₂Cl₂, 0.1 M TBAP is shown in Figure 4c. The assignment of a reduction or oxidation is based on RDE (rotating disc electrode) results which show a zero current at +0.10 V. The data is self consistent and a summary of the three electrode reaction involving Rh₂(ap)₄(O₂) is given by Eq. (2)-(4).

$$Rh_2(ap)_4(O_2) + e^- \rightleftarrows [Rh_2(ap)_4(O_2)]^- \qquad (2)$$

$$Rh_2(ap)_4(O_2) \rightleftarrows [Rh_2(ap)_4(O_2)]^+ + e^- \qquad (3)$$

$$[Rh_2(ap)_4(O_2)]^+ \rightleftarrows [Rh_2(ap)_4(O_2)]^{2+} + e^- \qquad (4)$$

Attempts were also made to characterize electrogenerated [Rh₂(ap)₄(O₂)]$^+$ and [Rh₂(ap)₄(O₂)]$^-$ by IR spectroscopy but unfortunately assignments for dioxygen or superoxide could not be made due to the presence of strong overlapping absorptions from the supporting electrolyte. On the other hand, the electrooxidized and electroreduced prodcuts are relatively stable for short time periods and the resulting ESR data on the products of the electrode reactions seems to be defi-

Table 1. ESR Data of Electrooxidized and Electroreduced $Rh_2(ap)_4$ Complex under an O_2 or Ar Atmosphere

Isomer	Electrogenerated compound	Solvent[a]	Atm[b]	Applied potential (V)	g_1	g_2	g_3 $(A_3 \times 10^4$ cm$^{-1})$	Ref.
2,2-*trans*	$[Rh_2(ap)_4(O_2)]^-$	THF	O_2	-0.65	2.09	2.02	1.99	tw
	$[Rh_2(ap)_4(O_2)]^-$	CH_2Cl_2	O_2	-0.65	2.06	2.02	1.97	tw
	$[Rh_2(ap)_4(CH_3CN)(O_2)]^-$	CH_3CN	O_2	-0.65	2.10	2.02	1.96	tw
	$[Rh_2(ap)_4]^+$	CH_2Cl_2	Ar	0.55	2.08	2.06	1.96 (15.6)	1
	$[Rh_2(ap)_4(CH_3CN)_2]^+$	CH_3CN	O_2	0.55	2.07	2.05	1.96 (17.4)	tw
	$[Rh_2(ap)_4(O_2)]^+$	CH_3Cl_2	O_2	0.55	2.10	2.07	1.96	tw
4,0	$[Rh_2(ap)_4(O_2)]^-$	CH_2Cl_2	O_2	-0.65	2.09	2.03	2.00	1
	$[Rh_2(ap)_4(O_2)]^-$	THF	O_2	-0.65	2.10	2.01	1.99	tw
					$g_\perp$	$g_\parallel$	$(A_\parallel \times 10^4$ cm$^{-1})$	
	$Rh_2(ap)_4Cl$	CH_2Cl_2	Ar	—	2.09	1.95 (26.4)		3
	O_2^-	THF	O_2	-0.65	2.01	2.01		tw

[a] Solution containing 0.1 M TBAP. [b] One atmosphere of gas. tw=this work.

nitive as discussed in the following section.

Spectroscopic Characterization of $[Rh^{II}_2(ap)_4(O_2)]^-$. ESR data for the 2,2-*trans* and 4,0 isomers of $Rh_2(ap)_4$ under different solution conditions are given in Table 1. The product generated after controlled potential reduction of the 2,2-*trans* isomer in CH_2Cl_2 under O_2 (Figuure 5a) has a rhombic signal with $g_1=2.06$, $g_2=2.02$ and $g_3=1.97$. No splitting due to Rh $(I=1/2)$ is observed and the spectrum indicates the formation of $[Rh_2(ap)_4(O_2)]^-$ where the odd electron is primarily located on the axially coordinated O_2. This implies the formation of a superoxide adduct. The ESR spectrum of the $[Rh_2(ap)_4(O_2)]^-$ 4,0 isomer is similar in shape to that of the 2,2-*trans* isomer, but the g values are slightly different (see Table 1) due to the different geometric arrangements of the bridging ligands.

An ESR signal for free O_2^- is not observed after reduction of the 4,0 isomer of $Rh_2(ap)_4(O_2)$ in $CH_2Cl_2{}^3$ and this is expected since any generated superoxide ion would react with the solvent.[5,6] A free O_2^- signal is also not observed after reduction of the oxygen adduct of the 2,2-*trans* isomer in this solvent. There is a small signal at $g=2.12$ in Figure 5a (marked by an x). The source of this signal is not clear but there are several possibilities, one of which is a kind of trace species from $[Rh_2(ap)_4(O_2)]^-$ in solution. However, further discussions regarding the identity of the species responsible for this signal would be highly speculative at this time.

The addition of CH_3CN to CH_2Cl_2 solutions of $[Rh_2(ap)_4(O_2)]^-$ leads to a new ESR spectrum with $g_1=2.10$, $g_2=2.02$ and $g_3=1.96$. This spectrum is shown in Figure 5b and is attributed to $[Rh_2(ap)_4(O_2)(CH_3CN)]^-$, where CH_3CN is coordinated *trans* to the bound dioxygen ligand.

Cyclic voltammograms of $Rh_2(ap)_4$ in neat CH_3CN under O_2 show no new reductions or oxidations. In addition, no rhodium-superoxide ESR signal is obtained, either during or after bulk controlled portential electroreduction of $Rh_2(ap)_4$ at -0.65 V in CH_3CN under O_2. This suggests that $Rh_2(ap)_4$ (CH_3CN) or $Rh_2(ap)_4(CH_3CN)_2$, rather than an O_2 adduct, is formed in neat CH_2CN.

The ESR spectrum of the product after reduction of Rh_2 $(ap)_4$ at -0.65 V in THF containing O_2 is shown in Figure 6b and appears to be a combination of overlapped signals

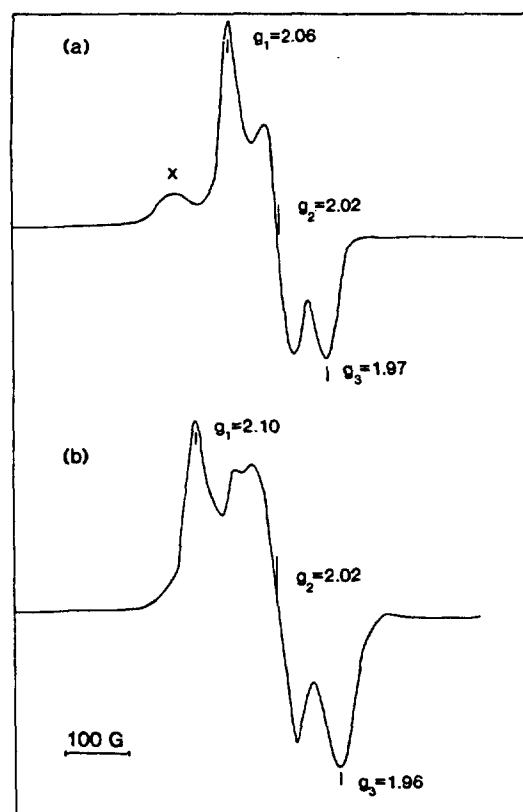**Figure 5.** ESR spectra obtained at 123 K after controlled potential reduction of $Rh_2(ap)_4$ in CH_2Cl_2, 0.1 M TBAP (a) under O_2 and (b) under O_2 in solutions containing 1 M CH_3CN. Applied potential= -0.65 V.

from free O_2^- and $[Rh_2(ap)_4(O_2)]^-$. This was confirmed by ESR spectrum taken after bulk controlled potential electrolysis of free O_2 at -0.65 V in THF, 0.1 M TBAP (Figure 6a). The potential for O_2 reduction in THF is ~ -0.9 V but small amounts of O_2^- can still be generated at more positive potentials. The O_2^- spectrum in Figure 6a has an axial signal at $g_\parallel=2.10$ and $g_\perp=2.01$ and is similar to the ESR spectrum of O_2^- in DMSO $(g_\parallel=2.10$ and $g_\perp=2.01)^7$ or CH_2Cl_2-
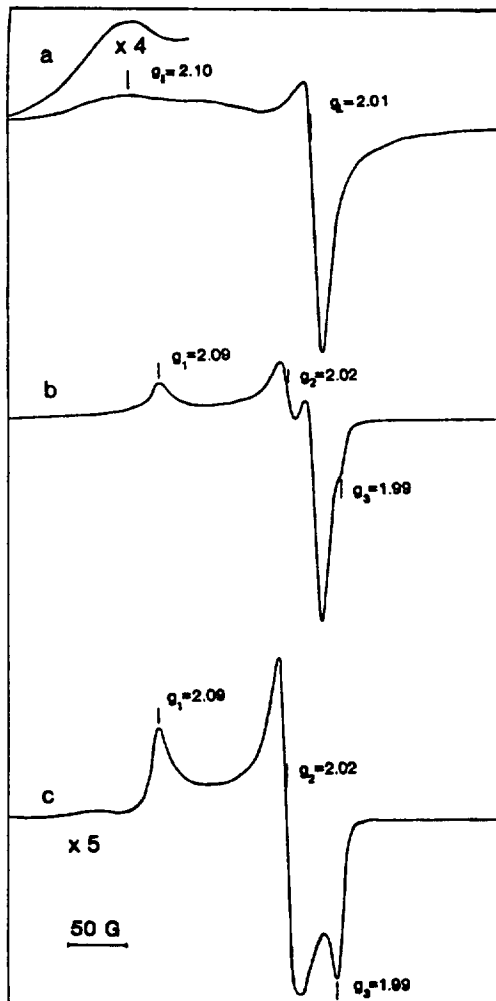
Figure 6. ESR spectra obtained at 123 K after controlled potential reduction of (a) O_2 in THF at -0.65 V, (b) $Rh_2(ap)_4$ in THF under O_2 at -0.65 V and (c) $Rh_2(ap)_4(O_2)$ in THF under O_2 at -0.25 V after bulk electrolysis at -0.65 V.

Figure 7. ESR spectra obtained at 123 K after controlled potential oxidation of $Rh_2(ap)_4$ (a) in CH_2Cl_2 and (b) in CH_2Cl_2 containing 5×10^{-3} M CH_3CN. Applied potential$=0.55$ V under O_2.

acetone-methanol mixtures.[4,8]

The ESR spectrum in Figure 6c is obtained from an initial solution $Rh_2(ap)_4(O_2)$ in THF under O_2 when the controlled potential is stepped to -0.25 V after bulk electrolysis at -0.65 V. This spectrum, with $g_1=2.09$, $g_2=2.02$, and $g_3 = 1.99$, is due to $[Rh_2(ap)_4(O_2)]^-$ which had not been completely reoxidized at a potential of -0.25 V. The ESR spectrum in Figure 6c is similar to the 4,0 isomer $[Rh_2(ap)_4(O_2)]^-$ which has a spectrum with signals at $g_1=2.10$, $g_2=2.01$ and $g_3=1.99$ (see Table 1).

Spectroscopic Characterization of $[Rh_2(ap)_4(O_2)]^+$. Figure 7a shows the ESR spectrum obtained after a bulk, controlled potential one-electron oxidation of $Rh_2(ap)_4$ in CH_2Cl_2 under O_2. The spectrum has an asymetric signal at $g_1=2.10$, $g_2=2.07$ and $g_3=1.96$ and clearly indicates the formation of $[Rh_2(ap)_4(O_2)]^+$. The g_3 value is the same as the g_3 of $[Rh_2-(ap)_4]^+$ in CH_2Cl_2 under Ar (see Table 1) but the signal is not split by the two Rh nuclei. This spectrum might be assigned as that of a formal $[Rh^{III}_2(ap)_4(O_2)]^+$ species which has axially bound superoxide ion, but is probably better described $[Rh^{II}Rh^{III}(ap)_4(O_2)]^+$, which has axially coordinated
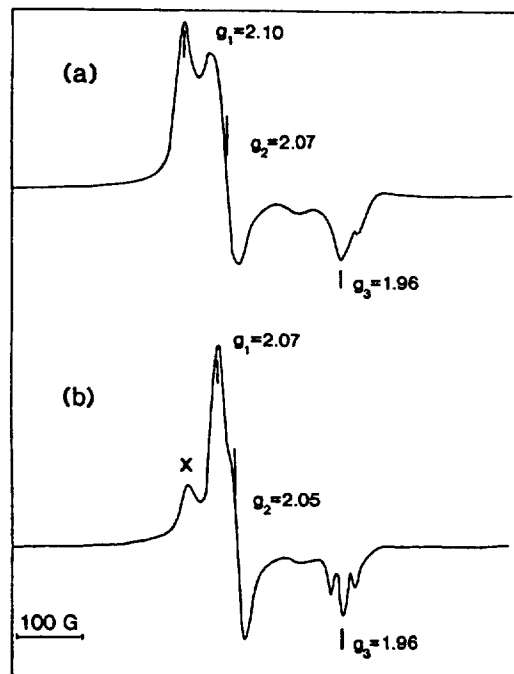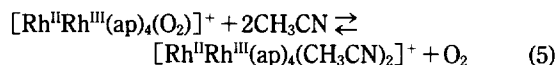
dioxygen.

Support for a dioxygen assignment is given by the ESR spectrum of electrooxidized $Rh_2(ap)_4$ in CH_2Cl_2 containing 5×10^{-3} M CH_3CN under O_2 (see Figure 7b). Some $[Rh_2(ap)_4 (O_2)]^+$ remains in solution (marked as x in Figure 7b). However, the stronger signals at $g_1=2.07$, $g_2=2.05$ and $g_3=1.96$ (a $1:2:1$ triple) clearly indicate the formation of a dirhodium(II, III) complex which is similar to $[Rh_2(ap)_4]^+$ (see Table 1) and does not contain bound molecular oxygen. These spectral data thus suggest the occurrence of reaction 5 upon addition of CH_2CN to CH_2Cl_2 solutions of $[Rh_2(ap)_4-(O_2)]^+$.

$$[Rh^{II}Rh^{III}(ap)_4(O_2)]^+ + 2CH_3CN \rightleftarrows$$
$$[Rh^{II}Rh^{III}(ap)_4(CH_3CN)_2]^+ + O_2 \qquad (5)$$

In summary, O_2 or O_2^- adducts may be formed with dirhodium complexes in formal Rh^{II}_2, $Rh^{II}Rh^{III}$ and Rh^{III}_2 oxidation states. $Rh_2(ap)_4$ react with dioxygen to form $Rh_2(ap)_4(O_2)$, and this species can undergo a metal centered one-electron reduction to produce $[Rh_2(ap)_4(O_2)]^-$ or a metal centered one-electron oxidation to produce $[Rh_2(ap)_4(O_2)]^+$. The three complexes all differ in the formal oxidation state of the dirhodium unit and consequently all three show a different degree of dioxygen interaction.

References

1. J. L. Bear, C.-L. Yao, L.-M. Liu, F. J. Capdevielle, J. D.

Korp, T. A. Albright, S.-K. Kang, and K. M. Kadish, *Inorg. Chem.*, **28**, 1254 (1989).

2. J. L. Bear, L.-M. Liu, and K. M. Kadish, *Inorg. Chem.*, **26**, 2927 (1987).

3. J. L. Bear, C.-L. Yao, F. J. Capdevielle, and K. M. Kadish, *Inorg. Chem.*, **27**, 3782 (1988).

4. K. Nakamoto, "Infrared and Raman Spectra of Inorganic and Coordination Compounds", Wiley-Interscience: New York, 4th edition, (1986).

5. J. T. Creager, S. A. Raybuck, and R. W. Murray, *J. Am. Chem. Soc.*, **108**, 4225 (1986).

6. J. L. Roberts, Jr. and D. T. Sawyer, *J. Am. Chem. Soc.*, **103**, 712 (1981).

7. H. Sakurai, K. Ishizu, and K. Okada, *Inorg. Chim. Acta*, **91**, L9 (1984).

8. P. Mourenot, J. Demuynck, and M. Benard, *Chem. Phys. Letts.*, **136**, 279 (1987).

Two Polymorphs of Structures of α,α-Trehalose Octaacetate Monohydrate

Young Ja Park* and Jung Mi Shin

Department of Chemistry, Sook Myung Women's University, Seoul 140-742

Structures of two polymorphs of α,α-trehalose octaacetate monohydrate, $C_{28}H_{38}O_{19} \cdot H_2O$, have been studied by X-ray diffraction method. α,α-trehalose (α-D-glucopyranosyl α-D-glucopyranoside) is a nonreducing disaccharide. The polymorph I belongs to the monoclinic $P2_1$, and has unit cell parameters of $a = 10.725(1)$, $b = 15.110(4)$, $c = 11.199(5)$ Å, $\beta = 108.16(2)°$ and $Z = 2$. The polymorph II is orthorhombic $P2_12_12_1$, with $a = 13.684(4)$, $b = 15.802(4)$, $c = 17.990(9)$ Å and $Z = 4$. The final R and R_w values for monoclinic polymorph I are 0.043 and 0.048 and for orthorhombic polymorph II are 0.116 and 0.118, respectively. Those R values of polymorph II are high because the large thermal motions of acetyl groups and the poor quality of the crystal. The molecular conformations in the two polymorphs are similar. Both D-glucopyranosyl rings have chair $^4C_1$ conformations and atoms of glycosidic chain α(1→1) linkage are coplanar. The primary acetate groups of the pyranose residues assume both gauche-*trans* conformations. The molecules of two polymorphs have pseudo-C_2 symmetry at glycosidic O(1) atom. The bond lengths and angles are normal compared with those in other acetylated sugar compounds. The molecules in the monoclinic crystal are held by the hydrogen bonds with the water molecules and by van der Waals forces.

Introduction

α,α-trehalose octaacetate, $C_{28}H_{38}O_{19}$ is a acetylated product of α,α-trehalose which is a nonreducing symmetrical disaccharides composed of two glucosyl residues bridged by an α(1→1) linkage. α,α-trehalose derives its name from the trehala manna which forms the cocoons of a beetle of the *Laurinus* family. α,α-trehalose is relatively inert compared to many carbohydrates due to its nonreducing nature and stable glycosidic linkage, which is possibly why it has transport functions in some organisms[1].

X-ray crystal structure determinations of anhydrous α,α-trehalose[2], α,α-trehalose dihydrate[3,4] and α,α-trehalose calcium bromide monohydrate[5] have been already carried out.

The prime aim in this study is to examine the distortion of the ring arising from the introduction of the acetyl substituents, the variation of the conformation angles about the linkage oxygen and the molecular packing due to the suppression of the intra- and intermolecular hydrogen bonds which are present in the peracetylated crystal structure.

Experimental

2,3,4,6-tetra-O-acetyl-1-O-(2,3,4,6-tetra-O-acetyl-α-D-gluco-pyranosyl)-α-D-glucopyranose(α,α-trehalose octaacetate) from Sigma Chemical Company crystallized as two polymorphs; the stable monoclinic and unstable orthorbombic form. The monoclinic crystals were obtained by slow evaporation from a mixture of an aqueous ethyl ether and cyclohexane (polymorph I). The orthorhombic crystals were grown by evaporation of an aqueous methanolic solution. But this crystal decomposes very easily in the air. Therefore the orthorhombic crystal was mounted on a thin-walled lead-free capillary (polymorph II).

X-ray measurements of the two polymorphs were performed on an Nonius CAD-4 diffractometer. The most relevant data collection parameters are reported in Table 1. The intensity data of the orthorhombic form showed crystal damage during the data collection, and therefore were corrected as indicated by 14% intensity decrease of the standard reflection. Intensities were corrected for Lorentz and polarization factors, but absorption was ignored.

The structures of two polymorphs were solved by direct methods of the program Shelxs-86[6], and refined by Fourier and least-squares methods using Shelx-76[6] program.

The parameters of the monoclinic polymorph I refined were the positional parameters of all atoms, anisotropic thermal parameters for nonhydrogen atoms and isotropic thermal